Synergistic Catalytic Effects of Alloys of Noble Metal Nanoparticles Supported on Two Different Supports

Asgar Pour, Zahra; Abduljawad, Marwan M.; Alassmy, Yasser A.; Alnafisah, Mohammed S.; El Hariri El Nokab, Mustapha; Van Steenberge, Paul H.M.; Sebakhy, Khaled O.

Published in:
Catalysts

DOI:
10.3390/catal13121486

Publication date:
2023

catalysts

MDPI

Article

Synergistic Catalytic Effects of Alloys of Noble Metal Nanoparticles Supported on Two Different Supports: Crystalline Zeolite Sn-Beta and Carbon Nanotubes for Glycerol Conversion to Methyl Lactate

Zahra Asgar Pour [1], Marwan M. Abduljawad [2], Yasser A. Alassmy [2], Mohammed S. Alnafisah [2], Mustapha El Hariri El Nokab [3], Paul H. M. Van Steenberge [4] and Khaled O. Sebakhy [4,*]

[1] Research and Development Department, Kisuma Chemicals, Billitonweg 7, 9641 KZ Veendam, The Netherlands; asgarpour@kisuma.com
[2] King Abdulaziz City for Science and Technology (KACST), Riyadh 11442, Saudi Arabia; mabduljawad@kacst.edu.sa (M.M.A.); yalassmy@kacst.edu.sa (Y.A.A.); malnafisah@kacst.edu.sa (M.S.A.)
[3] Zernike Institute for Advanced Materials (ZIAM), University of Groningen, Nijenborgh 4, 9747 AG Groningen, The Netherlands
[4] Laboratory for Chemical Technology (LCT), Department of Materials, Textiles and Chemical Engineering, Ghent University, Technologiepark 125, 9052 Ghent, Belgium; paul.vansteenberge@ugent.be
* Correspondence: khaled.sebakhy@ugent.be; Tel.: +32(0)-496764493

Abstract: Two multifunctional catalytic systems comprising Sn-based/doped crystalline zeolite Beta were synthesized, and they were employed as heterogeneous catalysts in the selective conversion of glycerol to methyl lactate. The first catalytic system, named Au-Pd-Sn-deAl-7.2-Beta-DP, was created through the post-synthesis dealumination of the parent zeolite Beta (Si/Al = 10) using 7.2 M HNO_3. Subsequently, it was grafted with 27 mmol of $SnCl_4$, resulting in Sn-deAl-7.2-Beta. Following this, Au and Pd nanoparticles were supported on this catalyst using the deposition–precipitation (DP) method. The second catalytic system was a physical mixture of Au and Pd nanoparticles supported on functionalized carbon nanotubes (Au-Pd-F-CNTs) and Sn-containing zeolite Beta (Sn-deAl-7.2-Beta). Both catalytic systems were employed in glycerol partial oxidation to methyl lactate under the following conditions: 140 °C for 4.5 h under an air pressure of 30 bar. The Au-Pd-Sn-deAl-7.2-Beta-DP catalytic system demonstrated 34% conversion of glycerol with a 76% selectivity for methyl lactate. In contrast, the physical mixture of Au-Pd-F-CNTs and Sn-deAl-7.2-Beta exhibited higher activity, achieving 58% glycerol conversion and a nearly identical selectivity for methyl lactate (77%). The catalytic results and catalyst structure were further analyzed using various characterization techniques, such as X-ray diffraction (XRD), N_2 physisorption, scanning electron microscopy (SEM), X-ray fluorescence (XRF), transmission electron microscopy (TEM), UV-vis spectroscopy, and pyridine Fourier transform infrared (FTIR). These analyses emphasized the significance of adjusting the quantity of active sites, particle size, and active sites proximity under the chosen reaction conditions.

Keywords: Sn-Beta zeolite; Lewis acid zeolites; multifunctional catalytic systems; gold alloy; glycerol conversion; methyl lactate

Citation: Asgar Pour, Z.; Abduljawad, M.M.; Alassmy, Y.A.; Alnafisah, M.S.; El Hariri El Nokab, M.; Van Steenberge, P.H.M.; Sebakhy, K.O. Synergistic Catalytic Effects of Alloys of Noble Metal Nanoparticles Supported on Two Different Supports: Crystalline Zeolite Sn-Beta and Carbon Nanotubes for Glycerol Conversion to Methyl Lactate. *Catalysts* **2023**, *13*, 1486. https://doi.org/10.3390/catal13121486

Academic Editor: Leonarda Liotta

Received: 21 October 2023
Revised: 22 November 2023
Accepted: 24 November 2023
Published: 30 November 2023

1. Introduction

Recently, the catalytic conversion of biomass compounds into biofuels has been considered one of the main academic topics related to the production of green energy resources. This trend is driven by the depletion of fossil fuel sources [1,2]. Given the limited available fossil fuel reservoirs, as well as global warming issues, biomass upgrading (e.g., agricultural crops and domestic food waste) is an alternative route for energy production. Bio-based materials are renewable carbon feedstocks, in contrast to petroleum-based fuels, and thus sustainable suppliers for generating energy [3,4]. In addition, due to the CO_2 adsorption

capacity and modern technologies developed for carbon capture from biomass, these materials contribute less to greenhouse gas emissions [5,6]. In this framework, biodiesel can be synthesized from biomass (e.g., animal fats or vegetable oils) to generate energy from these types of renewable feedstocks. However, extra glycerol is the main byproduct of biodiesel manufacturing, with a 10 wt.% production. Therefore, it needs to be valorized to more useful chemicals to prevent its surplus in the market [7]. The production of triose intermediates (i.e., 1,3 dihydroxyacetone (DHA) and glyceraldehyde (GLAD)) using the partial oxidation of glycerol is one of the several catalytic pathways used to consume excess glycerol. In the presence of alcohols, triose intermediates can be further converted into biodegradable alkyl lactates, which are applicable as green solvents and as precursors for the synthesis of biodegradable polymers (Scheme 1) [8]. To obtain these alkyl lactates from glycerol, the design of appropriate heterogeneous catalysts is a key step and thus crucial. To date, a variety of heterogeneous catalysts possessing both Brønsted and Lewis acid metals (Al, Sn, Zr, Hf, etc.) have been developed for the conversion of trioses to lactate [9,10]. However, the one-pot synthesis of alkyl lactates from glycerol using a heterogeneous catalyst possessing all of the required active sites is more intricate due to the complex reaction network and the possibility of the formation of several byproducts, which is the focus of our study as well [11–14]. Amongst the different heterogeneous catalysts, zeolite Beta, owing to several prominent properties, such as its crystalline structure, high surface area, large and channel-type pores, high Si/Al molar ratio, tunable Brønsted and Lewis acid sites, and high degrees of hydrophobicity, resulting in a water-resistant nature against the aqueous reaction medium, is a potential candidate for the conversion of trioses to lactates and, in combination with other catalysts, applicable for glycerol conversion to lactates [13,15–17].

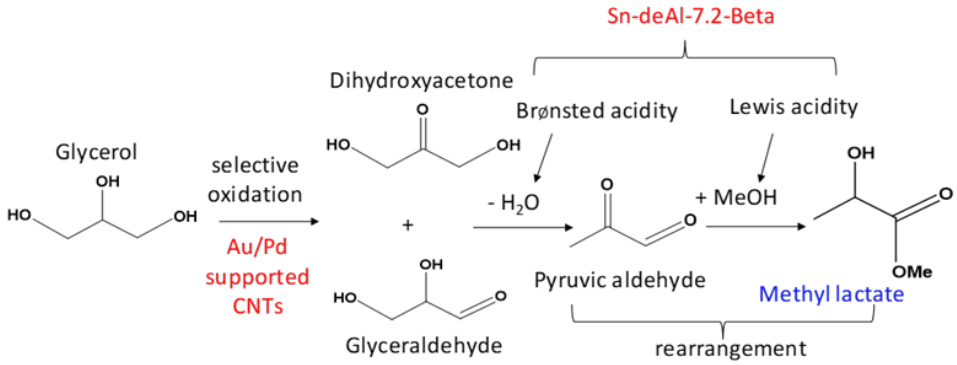

Scheme 1. Catalytic route for glycerol conversion to methyl lactate (ML) in the presence of methanol.

From a preparation standpoint, Sn-containing zeolite Beta is synthesized by incorporating Sn species into the zeolite matrix using classical hydrothermal synthesis in both hydroxide and fluoride media as mineralizing agents. However, using this approach requires a long synthesis time to obtain the crystalline Sn-Beta zeolite. To reduce the synthesis time, seeding techniques have also been employed to provoke the formation of new nuclei and the further growth of the crystallization center, and shortening the long synthesis time [18–20]. Nevertheless, the application of a highly corrosive and environmentally noxious F^- medium, as well as the long synthesis time required for hydrothermal crystallization, necessitates the investigation of alternative approaches, such as post-synthesis dealumination [21,22]. This is followed by Sn incorporation, mainly through the dissolution of the Sn precursor in an alcohol, and then Sn grafting into the zeolite framework [23]. Dealumination can be performed at various levels by using different concentrations of dealumination agents (e.g., inorganic or organic acids) to maintain an adequate amount of Al in the framework to conduct the dehydration step (see Scheme 1) [23,24]. In addition to using dealumination and further metal grafting, the use of the F^- medium can be avoided in post synthesis method. Apart from this advantage, due to the simple procedure, post-synthesis technique has also shown a practical potential for scale-up purposes [25,26]. The next step

is the implementation of oxidation catalytic centers (e.g., Au and Pd nanoparticles) on the prepared Sn-containing Beta as the catalytic support. Several heterogeneous oxidation catalysts have been reported for the selective oxidation of glycerol, such as platinum (Pt) or gold (Au) supported on carbon nanotubes [27,28].

To expand the scope of active heterogeneous catalysts facilitating the one-pot conversion of glycerol to methyl lactate, our prior research focused on developing a new catalytic system to conduct this reaction. This system employed Au and Pd nanoparticles supported on carbon nanotubes, combined in a physical mixture with spherically shaped Sn-zeolite Beta [17]. The synthesis of Sn-Beta beads involved a hard-templating technique, enabling the creation of hierarchical porosity and shaped zeolite Sn-Beta, concurrently [29]. However, this particular catalytic system exhibited only moderate activity in the targeted reaction, prompting the further exploration of new catalytic systems [17]. To advance the catalytic properties of the newly developed catalysts and maximize their efficacy in converting glycerol to methyl lactate, we investigated the influence of the particle size and dispersibility of zeolite Sn-Beta powder compared to spherically shaped Sn-Beta on the catalytic performance. Hence, we pursued two synthetic strategies: (i) a physical mixture involving Au and Pd nanoparticles supported on functionalized carbon nanotubes paired with crystalline, finely particulate Sn-Beta powder—comprising two distinct catalytic components—and (ii) multifunctional zeolite Beta powder housing all catalytic centers integrated within a single crystalline support. This strategy allowed us to examine the effect of the proximity of various catalytic centers supported on a singular material (i.e., zeolite Beta) on the final catalytic performance in the one-pot conversion of glycerol to methyl lactate. The synergy among diverse catalytic sites—Au and Pd nanoparticles facilitating the partial oxidation of glycerol, and Al and Sn acting as Brønsted and Lewis acid sites for dehydration and rearrangement reactions, respectively—exerts a cooperative effect, inhibiting the formation of side products resulting from cascade reactions. Additionally, the introduction of less-reactive metals such as Sn influences both the nucleation and growth steps in the hydrothermal crystallization of zeolite Beta, potentially complicating the preparation of the pure zeolite Beta phase [30,31]. Addressing these challenges and facilitating Au and Pd grafting onto the surface of crystalline zeolite Sn-Beta involved a multi-step procedure. Initially, the parent Beta powder underwent partial dealumination using HNO_3, followed by the introduction of Sn atoms through a straightforward grafting protocol [23]. Subsequently, Au and Pd nanoparticles were supported on Sn-containing Beta using a deposition–precipitation method [32]. In the alternative catalytic system, Au and Pd were supported on the surface of functionalized carbon nanotubes and combined with Sn-Beta zeolite as a physical mixture of two catalytic samples. Both catalytic systems were then evaluated in the one-pot glycerol conversion to methyl lactate, and their catalytic performance was meticulously compared to assess their efficiency in this reaction. The results of the catalytic reactions highlighted the advantageous effects of the proximity of different catalytic samples, including enhanced catalytic performance and the suppression of side-product formation.

2. Results and Discussion

Two distinct catalytic systems were devised and assessed for their efficacy in conducting the conversion of glycerol to methyl lactate: a multifunctional zeolite Beta, denoted by Au-Pd-Sn-deAl-7.2-Beta-DP, and a combination of physically mixed Au-Pd-F-CNTs with Sn-deAl-7.2 Beta. In the case of the first zeolite type, all catalytic centers were consolidated within the crystalline zeolite Beta as a unified support, allowing for an exploration of the influence of proximity among various catalytic active sites embedded within a single crystalline structure. The combined action of Au and Pd nanoparticles proved advantageous for the partial oxidation of glycerol [33]. The Lewis acidity emanating from Sn atoms grafted in silanol nests synergized with the Brønsted acidity originating from the framework Al^{+3}, linked to H^+ via an oxygen bridge. As illustrated in Scheme 1, Brønsted acidity catalyzes the triose dehydration step, while Lewis acidity facilitates the rearrangement step by in-

ducing a hydride shift, ultimately yielding methyl lactate from the intermediate pyruvic aldehyde [23]. The second catalytic system was formulated based on the catalytic outcomes derived from our previously developed catalyst, comprising Au-Pd supported on CNTs and shaped Sn-deAl-7.2-Beta beads. This system aimed to assess the impact of highly dispersed crystalline Sn-containing zeolite Beta and noble metals supported on CNTs in the one-pot conversion of glycerol to methyl lactate [17].

The XRD measurement of Sn-containing powder (Figure 1) showed the preserved crystalline structure after acid treatment and Sn grafting. Furthermore, traces of SnO_2, which is an inactive species in this reaction, were observed in both samples, and together with other measurements (see UV-Vis and catalytic results section), this indicates that the main part of Sn was incorporated into the tetrahedral coordination inside the zeolitic framework. The presence of minor amounts of crystalline SnO_2 in zeolite samples is presumably due to the residual species of Sn that remained after the washing step, which can be converted to SnO_2 after the second calcination step. As can be seen, the first and second main characteristic peaks of zeolite Beta appeared at approximately $2\theta = 7.5^\circ$ and 22.5°, which indicates that the presence of Sn in the structure did not alter the crystallinity and did not result in any shifts in the characterization peaks of zeolite Beta. Furthermore, for other peaks (e.g., with crystal lattice planes of 110, 101, 200, and 211), there is an overlap between zeolite Beta peaks and SnO_2. Accordingly, it is concluded that the formed amount of SnO_2, if any, is negligible.

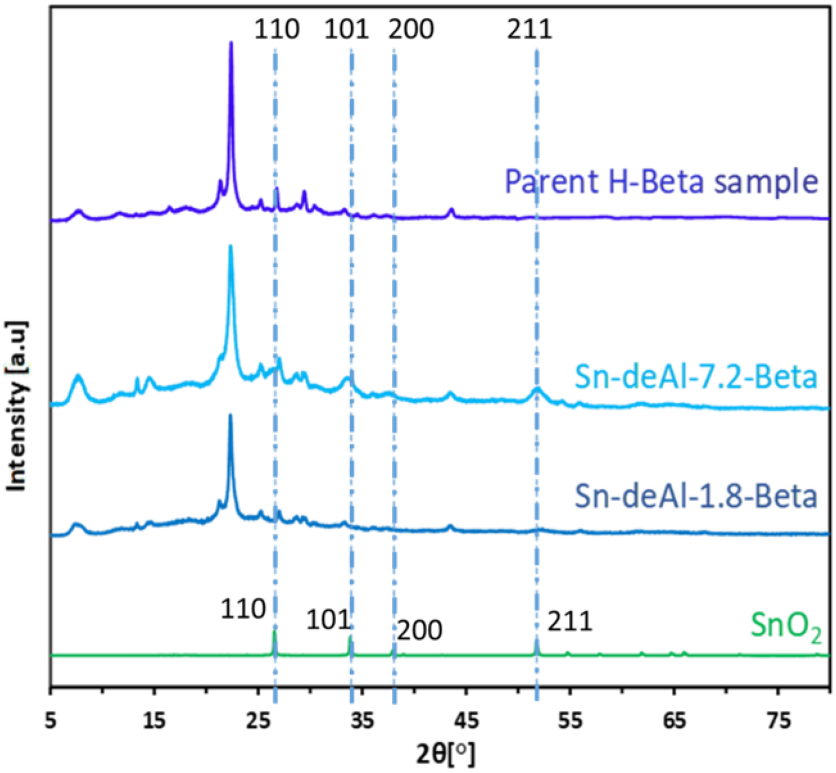

Figure 1. XRD patterns of Sn-containing Beta prepared with different acid concentrations (1.8 and 7.2 M HNO_3) and 27 mmol of $SnCl_4$. The presence of traces of SnO_2 was observed in both Sn-containing samples.

In SEM images, the Sn-containing zeolites displayed morphological features like those reported in the literature (Figure 2), which showed a round-shape geometry due to the agglomeration of particles [23,34].

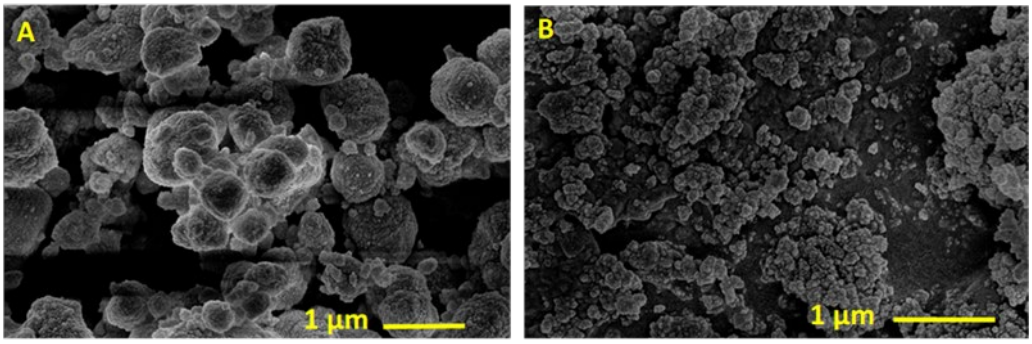

Figure 2. SEM images of (**A**) Sn-deAl-1.8-Beta and (**B**) Sn-deAl-7.2-Beta powders.

In addition, by increasing the concentration of HNO_3 from 1.8 to 7.2 M and grafting 27 mmol $SnCl_4$, an ascending trend was observed for the removed amount of Al, as well as the final surface area of the sample, the latter of which is due to the formation of more pores in the framework, as proved by N_2 physisorption (Table 1, Entries 1 and 2, and Figure 3).

Table 1. Physicochemical properties of Sn-containing powders.

Entry	Catalyst	Specific Surface Area (m^2/g) [a]	Micropore Volume (cm^3/g) [a]	Total Pore Volume (cm^3/g) [a]	Acid Conc. (M)	Si/Al Molar Ratio [b]	Si/Sn Molar Ratio [c]
1	Sn-deAl-1.8-Beta	465	0.18	0.28	1.8	87	48
2	Sn-deAl-7.2-Beta	507	0.15	0.83	7.2	131	108

[a] BET surface area measured by N_2 physisorption and [b,c] elemental analysis determined by XRF technique.

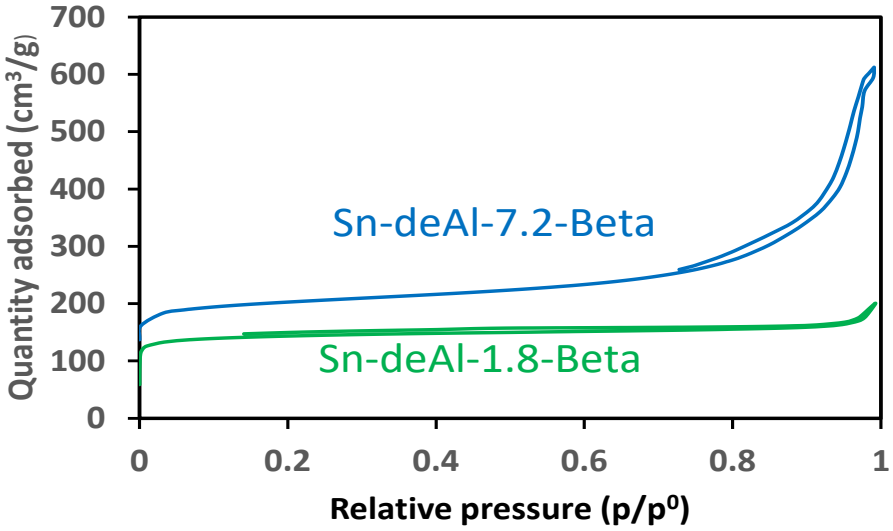

Figure 3. N_2 physisorption isotherms of Sn-deAl-1.8-Beta and Sn-deAl-7.2-Beta powders. For the sake of readability, the isotherm of Sn-deAl-7.2-Beta has been shifted up by 50 cm^3/g along the vertical axis.

The amount of metal incorporated into the zeolite matrix was measured using Diffuse Reflectance UV-Vis spectroscopy. In the UV-Vis spectra of the two Sn-containing zeolites, the band centered before the wavelength of 220 nm corresponds to the isolated Sn(IV) species in tetrahedral coordination (Figure 4A,B). Sn-deAl-7.2-Beta also displayed another broad shoulder with a weaker intensity at about 250 nm, which is representative of extra-framework Sn species in octahedral coordination, including both SnO_2 clusters and double-hydrated and isolated framework Sn(IV) (Figure 4B), which can be in the amorphous phase [24,35].

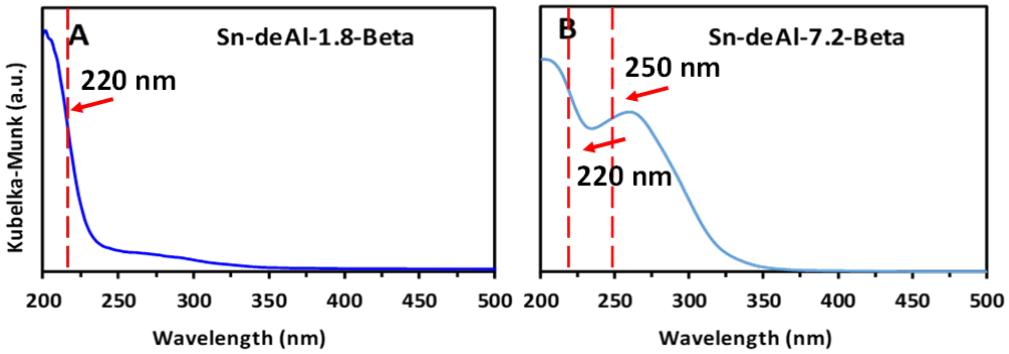

Figure 4. DR-UV-Vis spectra of Sn-containing zeolite Beta samples: (**A**) Sn-deAl-1.8-Beta and (**B**) Sn-deAl-7.2-Beta.

The type and strength of the acid sites in the two Sn-containing zeolites were evaluated by pyridine FT-IR temperature-programmed desorption (TPD). The intensities of signals centered at 1450 and 1540 cm^{-1} were used to assess the amounts of Lewis and Brønsted acid sites, respectively (Table 2) [36]. Sn-deAl-7.2-Beta showed a higher Lewis acid content (90 μmol/g). On the other hand, in Sn-deAl-1.8-Beta, the intensity of signals corresponding to Brønsted acid sites was higher, indicating the presence of more Al in the sample (39 μmol/g). However, the Lewis acid bands of this sample displayed lower intensities, suggesting less Sn content embedded inside the zeolite framework (15 μmol/g), which agrees with the presence of fewer silanol nests for Sn incorporation.

Table 2. Type and amount of surface acid sites of selected Sn-containing zeolites estimated by pyridine TPD-FT-IR.

Entry	Catalyst	Lewis Acidity (μmol/g)	Brønsted Acidity (μmol/g)	Lewis/Brønsted Ratio
		150 °C	150 °C	150 °C
1	Sn-deAl-1.8-Beta	15	39	3
2	Sn-deAl-7.2-Beta	90	9	10

A Comparison between the Activities of Two Catalytic Systems for the Synthesis of ML from Glycerol

As stated earlier, glycerol conversion to methyl lactate has the possibility of forming several byproducts. To maximize the amount of methyl lactate, the catalytic system should be designed accurately to suppress the formation of other undesired byproducts. The main byproducts of glycerol conversion to methyl lactate, which are detected by GC, are methyl pyruvate (MP), methyl glycolate (MGo), dimethyl oxalate (DMO), dimethyl tartronate (DMT), methyl glycerate, and 1,2 glycerol formal (1,2 GF, also known as solketal). The blended Sn-deAl-7.2-Beta and Au-Pd-F-CNTs catalysts displayed higher activity, with 58% conversion of glycerol and 77% selectivity for methyl lactate (Table 3, Entry 1), which is attributed to the generation of optimal amounts of Lewis and Brønsted acid sites for conducting the rearrangement reaction (measured by pyridine FTIR). The distribution and type of Sn sites (i.e., open or closed sites) are also influential, and it is likely that post-synthesis dealumination using 7.2 M HNO_3 introduces a lot of defects into the zeolite Beta crystalline network, which favors the formation of open Sn sites [37]. Furthermore, partially hydrolyzed open Sn sites (e.g., terminal Sn-OH), which are formed through the reaction of $SnCl_4$ with internal or surface silanols, are the most active species for methyl lactate synthesis owing to their higher basicity [35]. It is likely that a large population of these open Lewis acid sites was formed in Sn-deAl-7.2-Beta due to the application of a higher acid concentration, resulting in the formation of more defects and, consequently, a larger population of hydroxyl nests, which can embed open and active Sn atoms in defect

sites. In contrast, Sn-deAl-1.8-Beta, owing to different chemical compositions and the presence of more Al in the framework, has a more hydrophilic nature. Thus, it can be assumed that the deactivation of the catalytic system by adsorbing certain poisons, such as carboxylic acid, is more acute in this case [17]. In another catalytic test, we investigated the effect of the higher temperature on the catalytic activity of Sn-deAl-7.2-Beta, in which the reaction temperature increased to 155 °C (Table 3, Entry 2). Although glycerol conversion showed a 12% increase and reached 70%, the selectivity of methyl lactate decreased by 8%. In addition, a shift toward the formation of higher amounts of MGo and DMT was observed owing to the over-oxidation of the intermediate glyceraldehyde. The increase in the formation of 1,2 GF (solketal) in this test indicates that the rate of the acetalization reaction is higher at higher temperatures when strong Brønsted acid sites are present in zeolite and Sn functions as Lewis acid sites [38]. The prolongation of the reaction time to 10 h for both catalytic systems demonstrated an increase in the selectivity and yield of ML (Table 3, Entries 6 and 7); however, a higher conversion rate was only observed for Au-Pd-Sn-deAl-7.2-Beta-DP (65% vs. 29%), which is due to the further conversion of glycerol, while for the other catalytic system, the conversion curve likely reaches the plateau part after 5 h and then remains unchanged. The catalytic results of these samples compared with the previously reported shaped catalyst (Table 3, Entry 5) demonstrate that the degree of dispersion of catalysts is a very important parameter in maximizing the selectivity of methyl lactate in the reaction and minimizing the formation of other undesired byproducts that can be produced due to the over-oxidation of glycerol. The last sample tested in the conversion of glycerol to ML was Au-Pd-Sn-deAl-7.2-Beta-DP, which displayed similar selectivity to Sn-deAl-7.2-Beta (76%, Table 3, Entry 4) but lower glycerol conversion (34%). The TEM image of Au-Pd-F-CNTs (Figure 5A) demonstrates well-dispersed nanoparticles on carbon nanotubes with an average size of less than 10 nm estimated by visual screening and a wide particle size distribution, which is in agreement with the morphological properties previously reported for this catalyst and thus indicates the reproducibility of this synthesis technique [17]. In contrast, the direct use of Sn-deAl-7.2-Beta as a support for Au and Pd showed larger particles with less homogeneity in particle size and a lower density of metal loading (Figure 5B) using the DP method [32]. Because of the basic nature of the DP synthesis medium, the zeolite surface obtains negative charges, which, in turn, reduces the adsorption of negatively charged Au and Pd nanoparticles and thus decreases the efficiency of this technique for supporting noble metal nanoparticles on the zeolite surface. In addition to the lower adsorption quantities of Au and Pd, the weak interaction between these nanoparticles and the crystalline zeolite support leads to the formation of precipitated metal particles with a larger size but with a lower loading on the zeolitic support compared with carbon nanotubes [32]. On the other hand, the proximity of catalytic oxidation sites (i.e., Au and Pd nanoparticles) to the rearranged catalytic centers (protonated Al and Sn^{+4}) is probably the reason for the high selectivity of ML using this catalyst, but as stated before, due to the lower metal loading, the glycerol conversion is low (34%) using this catalyst. Altogether, the results obtained with these two catalytic systems reveal that an optimized and highly active catalytic system is a combination of a catalytic support having very fine noble metals in which all active sites are accommodated to suppress the formation of undesired byproducts.

Table 3. Catalytic performance of two catalytic systems.

Entry	Catalyst	Conv. (%)	Yield of ML (%)	Selectivity (%)							Ref.
				ML	MP	MGo	DMO	1,2 GF	DMT	MGe	
1	Sn-deAl-7.2-Beta + Au-Pd-F-CNTs	58	45	77	n.d.	8.6	2.7	2.4	n.d.	4.8	This work
2	Sn-deAl-7.2-Beta + Au-Pd-F-CNTs [a]	70	49	69	n.d.	12.6	0	6.1	7.1	4.5	This work
3	Sn-deAl-1.8-Beta + Au-Pd-F-CNTs	29	17	70	n.d.	8.2	0	16.9	n.d	4.9	This work
4	Au-Pd-Sn-deAl-7.2-Beta-DP [b]	34	26	76	n.d.	12.5	0	2.1	0.5	6.3	This work
5	Sn-deAl-1.8-Beta-B + Au-Pd-F-CNTs [c]	29	20	67	n.d.	5.8	4.8	5.8	7.1	3.9	[17]
6	Sn-deAl-7.2-Beta + Au-Pd-F-CNTs [d]	69	57	82	n.d.	0.1	0	11.1	3.5	3	This work
7	Au-Pd-Sn-deAl-7.2-Beta-DP [d]	65	50.7	78	n.d.	9	0	2	6	5	This work

Reaction conditions: 20 mL of glycerol 0.25 M in MeOH, 0.1 g of Au-Pd-F-CNTs, 0.2 g of Sn-containing zeolite, temperature = 140 °C, reaction pressure = 30 bar air, 4.5 h; [a]: run at 155 °C; [b]: for this reaction, only 0.2 g of Au-Pd-Sn-deAl-7.2-Beta-DP was used as catalyst (n.d. = not detected); [c]: spherically shaped catalysts (B: indicating bead-shaped catalytic particles) applied in the same reaction conditions as Ref. [17]; [d]: both reactions were run for 10 h.

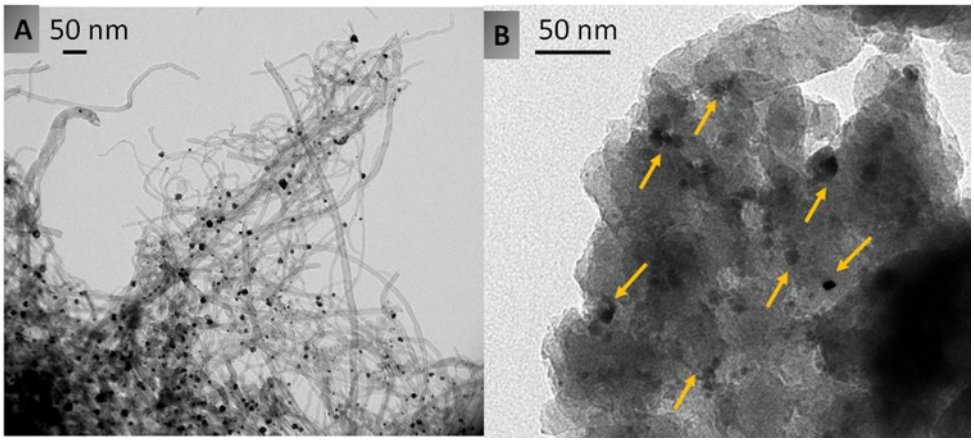

Figure 5. TEM image of (**A**) Au and Pd nanoparticles supported on functionalized carbon nanotubes (i.e., Au-Pd-F-CNTs) and (**B**) Au and Pd supported on active bimetallic Beta zeolite (i.e., Sn-deAl-7.2-Beta). The metal particles supported on zeolite Beta are shown with yellow arrows.

3. Experimental Section

3.1. Materials

Glycerol (99%), methyl glycolate (98%), methyl lactate (98%), tartronic acid (97%), di-methyl oxalate (99%), glyceric acid (20% in H_2O), methyl pyruvate (98%), tin chloride ($SnCl_4$, 98%), pyruvic aldehyde dimethyl actal (98%), tetraethylammonium hydroxide (TEAOH, 35 wt.% in H_2O), silica gel (high purity grade 9385), gold (III) chloride hydrate (99.999%), Palladium (II) chloride (99.999%), polyvinyl alcohol (PVA, MW 9000–10,000, 80% hydrolyzed), sodium borohydride (99%), nitric acid (ACS reagent 70 wt.%), and multi-walled carbon nanotubes (CNTs > 95% purity, O.D. (outer diameter) × L (length) 6–9 nm × 5 µm) were purchased from Sigma Aldrich (Louis, MO, USA). Sulfuric acid (98%) was purchased from Merck (Darmstadt, Germany). Sodium aluminate anhydrous (purity 99.5%) was purchased from Riedel-de Haën. MilliQ water was used for different steps of synthesis. All chemicals were used as received without further purification.

3.2. Catalyst Synthesis

First, the parent zeolite Beta sample was synthesized based on the original method developed for the preparation of this type of zeolite [39]. In a typical synthesis, 4.58 g

of silica gel was slightly dissolved in 17.71 g of tetraethylammonium hydroxide solution (TEAOH, 35 wt.% in H_2O) and stirred for 1 h at room temperature. Meanwhile, 0.57 g of $NaAlO_2$ was dissolved in 10.74 g of H_2O under stirring for 10 min, and then the transparent solution was added dropwise to the first solution and further stirred for 1 h. This mixture was hydrothermally treated in a static mode in a 50 mL Teflon-lined autoclave at 150 °C for 6 days. Then, the autoclave was cooled down to room temperature and opened, and the obtained zeolite Beta sample was washed with H_2O (1 L) to reach a pH of around 7–8 and dried at 100 °C overnight. The calcination step was carried out in a muffle furnace under static air with a two-step temperature program (3 °C/min from 20 °C to 200 °C, 6 h, 2 °C/min to 600 °C, 6 h). The obtained zeolite Beta powder after calcination was in the Na form and further ion-exchanged using 1 M NH_4NO_3 solution (10 mL/1 g of zeolite) under stirring at 80 °C for 8 h. After the ion-exchange step, the sample was dried and calcined with the above-mentioned calcination temperature program to give the protonated type of zeolite Beta powder possessing Brønsted acidity. To introduce tetrahedrally coordinated Sn species as Lewis acid centers into the zeolite structure, the parent zeolite powder was initially dealuminated using HNO_3 (1.8 M or 7.2 M, 55 mL/1 g zeolite) under stirring at 80 °C for 15 h. Following this step, samples were washed to remove Al residues and dried at 60 °C overnight [23]. The metal-grafting step was conducted by adding 1 g of dealuminated zeolite to 100 mL of Sn precursor (i.e., 0.27 M $SnCl_4$ dissolved in dried 1-propanol), and this mixture was stirred under a N_2 atmosphere with cooling water reflux for 7 h. Finally, the obtained product was washed with dry isopropanol, dried at 60 °C, and calcined with the above-mentioned temperature protocol.

Dealuminated and metal-grafted samples were labeled Sn-deAl-c-Beta, in which "c" is representative of the acid concentration (HNO_3 1.8 or 7.2 M). The Au and Pd nanoparticles were supported on functionalized CNTs with a total metal loading of 1 wt.% based on the colloidal immobilization method [17,33]. In a typical test, 1 g of CNTs was stirred with both HNO_3 (10 mL, 30 wt.%) and H_2SO_4 (10 mL, 98 wt.%) under reflux for 20 h at 350 rpm and 60 °C. Next, this suspension was filtered, washed, and dried overnight at 100 °C. This treatment was applied to guide highly dispersed nanoparticles onto the surface of CNTs (visualized by SEM; see discussion section). To anchor Au and Pd, a mixture of Au (1.85 mL, 0.018 M), Pd (1 mL, 0.033 M), and 1.2 mL PVA were added to 100 mL of H_2O and stirred at 800 rpm for 0.5 h at 25 °C. Next, 2.5 mL of basic $NaBH_4$ solution (0.1 M) was added gradually to this mixture as a reducing agent, and the mixture was stirred for the next 0.5 h under the same conditions. Afterward, the pH was reduced to 2 by adding 1 M H_2SO_4 dropwise to this mixture. Finally, 1 g of functionalized CNTs was added to this mixture, stirred for 2 h, washed to a pH of about 7, and dried at 100 °C overnight [17,33]. Furthermore, we synthesized another catalytic system via direct supporting of Au and Pd on highly active crystalline Sn-containing zeolite Beta (i.e., Sn-deAl-7.2-Beta) using the deposition–precipitation method, which was labeled AuPd-Sn27-deAl-7.2-Beta-P-DP [32]. In a typical synthesis, 2.44 g of urea and 1 g of Sn-containing zeolite were dissolved in 50 mL of H_2O. To this solution, 1.85 mL of an aqueous solution of $HAuCl_4$ (3.5 Au/L) and 1 mL of PdCl2.2HCl (3.5 g Pd/L) were added under stirring. The flask was fully covered with aluminum foil to be protected from light and stirred at 80 °C for 6 h. The obtained suspension was further stirred at room temperature for 12 h, washed with water, dried at 100 °C for 6 h, and thermally treated in a quartz tubular oven under a flowing air stream at 200 °C for 5 h [32]. This catalyst was labeled Au-Pd-Sn-deAl-7.2-Beta-DP.

3.3. Catalytic Tests

A 100 mL Parr stainless-steel autoclave equipped with a Teflon liner was used as a high-pressure reactor for the catalytic conversion of glycerol to ML. In a typical test, 20 mL of glycerol (0.25 M in methanol) with a physical mixture of 0.1 g of Au-Pd-F-CNTs and 0.2 g of Sn-containing zeolite Beta powders (i.e., Sn-deAl-7.2-Beta or Sn-deAl-1.8-Beta) were transferred to the reactor, and the reaction mixture was stirred using an overhead mechanical stirrer at 800 rpm under 30 bar pressure of air as the oxidizing agent for

5 h, including 0.5 h for heating up the mixture from ambient temperature to 140 °C [33]. In addition, we conducted this reaction with 0.2 g of our newly designed catalysts (i.e., Au-Pd-Sn-deAl-7.2-Beta-DP) possessing all active sites embedded in one support (i.e., crystalline zeolite Beta dealuminated with 7.2 M HNO_3, Sn-deAl-7.2-Beta) to see the effect of the crystalline support and the proximity of all active centers in conducting this reaction. At the end of the reaction, the autoclave was cooled down to ambient temperature and then depressurized. The mixture of catalysts was separated from the reaction solution by filtration, and the liquid phase was analyzed using a GC instrument (Thermo Tracer) equipped with a flame ionization detector (FID) and a Restek Stabilwax-DA column (30 m length, 0.32 mm ID, and 1 μm df). The glycerol conversion was calculated using Equation (1):

$$\text{Conv.} = \frac{gly_0 - gly}{gly_0} \times 100\% \quad (1)$$

where gly_0 and gly are the glycerol concentrations at the beginning and the end of the reaction, respectively. The selectivity of the products was calculated using Equation (2):

$$\text{S}_{\text{prod.}} = \frac{C_{prod}}{gly_0 - gly} \times 100\% \quad (2)$$

where C_{prod} is the concentration of each product detected by GC. The carbon balance (C %) was calculated by the summation of unreacted glycerol and the yields of products calculated from GC.

3.4. Catalyst Characterization Methods

The degree of crystallinity of the zeolite Beta powder was measured with the X-ray diffraction technique (XRD) using a Bruker D-8 Advance-Germany spectrometer with Cu-Kα radiation and λ = 1.5418 Å generated at 40 kV and 40 mA. The 2θ angle data were collected from 5 to 80° with a step size of 0.02° and a scan rate of 1°/min. The surface morphology was investigated by scanning electron microscopy (SEM) using a Philips XL30 ESEM FEG. Before SEM, zeolite samples were coated with gold to create a conductive surface. N_2 physisorption isotherms were measured at −196 °C using a Micrometrics ASAP 2420. The BET (Brunauer–Emmet–Teller) model was applied to determine the specific surface area. The UV-Vis spectra were measured using a JASCO 570 UV−Vis-NIR absorption spectrometer (Easton, MD, USA). Lewis and Brønsted acidity were measured by FT-IR spectra using pyridine as a probe molecule in a Bruker Vertex 70 spectrometer (Rheinstetten, Germany) equipped with a liquid-nitrogen-cooled mercury–cadmium–telluride (MCT) detector with 4 cm^{-1} resolution and 128 scans. The self-supported discs (approximately 30 mg and with a disc diameter of about 1 cm) were first pretreated at 400 °C under vacuum for 5 h to remove the adsorbed water and next cooled down to room temperature. During the cooling step, the background spectra were recorded at 25 °C. Next, samples were saturated with pyridine vapor at 20 mbar and 25 °C for 30 min and evacuated again for 30 min to remove the physisorbed pyridine. The evacuated samples were subjected to TPD at 150 °C for 30 min with a heating rate of 4 °C/min, and the FT-IR spectra were recorded in situ at this temperature. The elemental analysis was performed with the X-ray fluorescence technique (XRF) using PANalytical Epsilon 3XLE, and different elements were measured in their oxide forms. Transmission electron microscopy (TEM) images were taken using a CM12 (Philips) electron microscope operating at 120 keV. TEM samples were prepared by ultra-sonicating the catalyst in ethanol for 40 min. Next, one drop of the prepared solution was placed on a 400-mesh copper grid coated with carbon.

4. Conclusions and Future Perspectives

In this study, we developed two catalytic systems for glycerol conversion to methyl lactate. To prepare the first catalytic system, the parent zeolite powder in the H-form, which was synthesized using hydrothermal crystallization, was partially dealuminated to generate

silanol nests for the grafting of Sn atoms as Lewis acid centers. The main factor that should be precisely tuned to obtain a highly active Sn-containing Beta is the acid concentration used for the dealumination step to generate the optimal ratio of Lewis to Brønsted acidity which conducts different steps after glycerol partial oxidation (i.e., rearrangement reaction). Next, the oxidation catalyst was prepared by utilizing either carbon nanotubes or Sn-Beta as a support. Based on the observed catalytic results, the combination of Au-Pd-F-CNTs with Sn-deAl-7.2-Beta demonstrated to be the most active catalytic system for glycerol conversion to ML because of the application of 7.2 M, compared to 1.8 M HNO_3. This adjusted ratio produced the optimal Lewis and Brønsted acid quantities for the rearrangement reaction (in agreement with the literature results) [23]. On the other hand, Au-Pd-Sn-deAl-7.2-Beta-DP, due to the proximity of all catalytic active sites, is a "selective" catalyst for the synthesis of methyl lactate. However, improvements using other synthetic protocols for the efficient grafting of the oxidative metal (e.g., proper particle size as well as the amount of metal loading) on the zeolitic surface remain to be explored [40–43]. New synthetic techniques should enable us to graft metals with the appropriate size as well as an adequate population on the zeolite Beta surface. In addition, future perspectives entail that ^{27}Al solid-state NMR will be performed to check the Si/Al ratio before and after dealumination and to detect the integration of Sn particles into the framework [44]. Moreover, experiments will be carried out in a continuous-flow mode and not only in a batch mode, such as one-pot synthesis.

Author Contributions: Conceptualization, Y.A.A. and Z.A.P.; methodology, Y.A.A.; formal analysis, K.O.S. and P.H.M.V.S.; investigation, Z.A.P. and K.O.S.; resources, writing—original draft preparation, Z.A.P. and M.E.H.E.N.; writing—review and editing, M.M.A. and M.S.A.; visualization, Y.A.A.; supervision, K.O.S. All authors have read and agreed to the published version of the manuscript.

Funding: This research received no external funding.

Data Availability Statement: Data are contained within the article.

Acknowledgments: Khaled O. Sebakhy thanks the Laboratory for Chemical Technology (LCT).

Conflicts of Interest: The authors declare no conflict of interest.

References

1. Mardiana, S.; Azhari, N.J.; Ilmi, T.; Kadja, G.T. Hierarchical zeolite for biomass conversion to biofuel: A review. *Fuel* **2022**, *309*, 122119. [CrossRef]
2. Alonso, D.M.; Bond, J.Q.; Dumesic, J.A. Catalytic conversion of biomass to biofuels. *Green Chem.* **2010**, *12*, 1493–1513. [CrossRef]
3. Dapsens, P.Y.; Mondelli, C.; Pérez-Ramírez, J. Biobased chemicals from conception toward industrial reality: Lessons learned and to be learned. *ACS Catal.* **2012**, *2*, 1487–1499. [CrossRef]
4. Sheldon, R.A. Green and sustainable manufacture of chemicals from biomass: State of the art. *Green Chem.* **2014**, *16*, 950–963. [CrossRef]
5. Gustavsson, L.; Börjesson, P.; Johansson, B.; Svenningsson, P. Reducing CO_2 emissions by substituting biomass for fossil fuels. *Energy* **1995**, *20*, 1097–1113. [CrossRef]
6. Azar, C.; Lindgren, K.; Larson, E.; Möllersten, K. Carbon capture and storage from fossil fuels and biomass–Costs and potential role in stabilizing the atmosphere. *Clim. Chang.* **2006**, *74*, 47–79. [CrossRef]
7. Okoye, P.U.; Hameed, B.H. Review on recent progress in catalytic carboxylation and acetylation of glycerol as a byproduct of biodiesel production. *Renew. Sustain. Energy Rev.* **2016**, *53*, 558–574. [CrossRef]
8. Sun, P.; Ling, W.; Wang, H.; Huang, J.; Liao, Y.; Wang, C. Hierarchical zeolite with open tin sites stabilized by metal ions catalyze the conversion of polysaccharides to alkyl lactates. *Mol. Catal.* **2023**, *545*, 113226. [CrossRef]
9. Alonso, D.M.; Wettstein, S.G.; Dumesic, J.A. Bimetallic catalysts for upgrading of biomass to fuels and chemicals. *Chem. Soc. Rev.* **2012**, *41*, 8075–8098. [CrossRef]
10. Dusselier, M.; Van Wouwe, P.; Dewaele, A.; Makshina, E.; Sels, B.F. Lactic acid as a platform chemical in the biobased economy: The role of chemocatalysis. *Energy Environ. Sci.* **2013**, *6*, 1415–1442. [CrossRef]
11. Tang, B.; Wang, D.; Li, A.; Tang, H.M.; Yang, E.C.; Dai, W. Constructing core-shell structured Au/Snβ@ mesosilica composite for one-pot base-free conversion of glycerol to methyl lactate. *Microporous Mesoporous Mater.* **2023**, *347*, 112348. [CrossRef]
12. Dapsens, P.Y.; Mondelli, C.; Pérez-Ramírez, J. Design of Lewis-acid centres in zeolitic matrices for the conversion of renewables. *Chem. Soc. Rev.* **2015**, *44*, 7025–7043. [CrossRef] [PubMed]
13. Zhou, C.H.; Beltramini, J.N.; Fan, X.Y.; Lu, G.Q. Chemoselective catalytic conversion of glycerol as a biorenewable source to valuable commodity chemicals. *Chem. Soc. Rev.* **2008**, *37*, 527–549. [CrossRef] [PubMed]

14. Besson, M.; Gallezot, P.; Pinel, C. Conversion of biomass into chemicals over metal catalysts. *Chem. Rev.* **2014**, *114*, 1827–1870. [CrossRef] [PubMed]
15. Román-Leshkov, Y.; Moliner, M.; Labinger, J.A.; Davis, M.E. Mechanism of glucose isomerization using a solid lewis acid catalyst in water. *Angew. Chem. Int. Ed.* **2010**, *49*, 8954–8957. [CrossRef] [PubMed]
16. Gounder, R.; Davis, M.E. Monosaccharide and disaccharide isomerization over Lewis acid sites in hydrophobic and hydrophilic molecular sieves. *J. Catal.* **2013**, *308*, 176–188. [CrossRef]
17. Asgar Pour, Z.; Boer, D.G.; Fang, S.; Tang, Z.; Pescarmona, P.P. Bimetallic Zeolite Beta Beads with Hierarchical Porosity as Brønsted-Lewis Solid Acid Catalysts for the Synthesis of Methyl Lactate. *Catalysts* **2021**, *11*, 1346. [CrossRef]
18. Mal, N.K.; Ramaswamy, A.V. Synthesis and catalytic properties of large-pore Sn-β and Al-free Sn-β molecular sieves. *Chem. Commun.* **1997**, *8*, 425–426. [CrossRef]
19. Camblor, M.A.; Corma, A.; Valencia, S. Spontaneous nucleation and growth of pure silica zeolite-β free of connectivity defects. *Chem. Commun.* **1996**, *20*, 2365–2366. [CrossRef]
20. Van Grieken, R.; Martos, C.; Sánchez-Sánchez, M.; Serrano, D.P.; Melero, J.A.; Iglesias, J.; Cubero, A.G. Synthesis of Sn-silicalite from hydrothermal conversion of SiO_2-SnO_2 xerogels. *Microporous Mesoporous Mater.* **2009**, *119*, 176–185. [CrossRef]
21. Dijkmans, J.; Gabriëls, D.; Dusselier, M.; De Clippel, F.; Vanelderen, P.; Houthoofd, K.; Malfliet, A.; Pontikes, Y.; Sels, B.F. Productive sugar isomerization with highly active Sn in dealuminated β zeolites. *Green Chem.* **2013**, *15*, 2777–2785. [CrossRef]
22. Valtchev, V.; Majano, G.; Mintova, S.; Pérez-Ramírez, J. Tailored crystalline microporous materials by post-synthesis modification. *Chem. Soc. Rev.* **2013**, *42*, 263–290. [CrossRef] [PubMed]
23. Dijkmans, J.; Dusselier, M.; Gabriëls, D.; Houthoofd, K.; Magusin, P.C.M.M.; Huang, S.; Pontikes, Y.; Trekels, M.; Vantomme, A.; Giebeler, L.; et al. Cooperative catalysis for multistep biomass conversion with Sn/Al beta zeolite. *ACS Catal.* **2015**, *5*, 928–940. [CrossRef]
24. Tang, B.; Dai, W.; Wu, G.; Guan, N.; Li, L.; Hunger, M. Improved post synthesis strategy to Sn-beta zeolites as lewis acid catalysts for the ring-opening hydration of epoxides. *ACS Catal.* **2014**, *4*, 2801–2810. [CrossRef]
25. Verboekend, D.; Vilé, G.; Pérez-Ramírez, J. Hierarchical Y and USY zeolites designed by post-synthetic strategies. *Adv. Funct. Mater.* **2012**, *22*, 916–928. [CrossRef]
26. Sun, H.; Peng, P.; Wang, Y.; Li, C.; Subhan, F.; Bai, P.; Xing, W.; Zhang, Z.; Liu, Z.; Yan, Z. Preparation, scale-up and application of meso-ZSM-5 zeolite by sequential desilication–dealumination. *J. Porous Mater.* **2017**, *24*, 1513–1525. [CrossRef]
27. Liang, D.; Gao, J.; Sun, H.; Chen, P.; Hou, Z.; Zheng, X. Selective oxidation of glycerol with oxygen in a base-free aqueous solution over MWNTs supported Pt catalysts. *Appl. Catal. B Environ.* **2011**, *106*, 423–432. [CrossRef]
28. Rodrigues, E.G.; Carabineiro, S.A.; Delgado, J.J.; Chen, X.; Pereira, M.F.; Órfão, J.J. Gold supported on carbon nanotubes for the selective oxidation of glycerol. *J. Catal.* **2012**, *285*, 83–91. [CrossRef]
29. Asgar Pour, Z.; Abduljawad, M.M.; Alassmy, Y.A.; Cardon, L.; Van Steenberge, P.H.M.; Sebakhy, K.O. A Comparative Review of Binder-Containing Extrusion and Alternative Shaping Techniques for Structuring of Zeolites into Different Geometrical Bodies. *Catalysts* **2023**, *13*, 656. [CrossRef]
30. Asgar Pour, Z.; Alassmy, Y.A.; Sebakhy, K.O. A Survey on Zeolite Synthesis and the Crystallization Process: Mechanism of Nucleation and Growth Steps. *Crystals* **2023**, *13*, 959. [CrossRef]
31. Asgar Pour, Z.; Sebakhy, K.O. A Review on the Effects of Organic Structure-Directing Agents on the Hydrothermal Synthesis and Physicochemical Properties of Zeolites. *Chemistry* **2022**, *4*, 431–446. [CrossRef]
32. Ma, Z.; Dai, S. Development of novel supported gold catalysts: A materials perspective. *Nano Res.* **2011**, *4*, 3–32. [CrossRef]
33. Tang, Z.; Boer, D.G.; Syariati, A.; Enache, M.; Rudolf, P.; Heeres, H.J.; Pescarmona, P.P. Base-free conversion of glycerol to methyl lactate using a multifunctional catalytic system consisting of Au–Pd nanoparticles on carbon nanotubes and Sn-MCM-41-XS. *Green Chem.* **2019**, *21*, 4115–4126. [CrossRef]
34. Wang, J.; Okumura, K.; Jaenicke, S.; Chuah, G.K. Post-synthesized zirconium-containing Beta zeolite in Meerwein-Ponndorf-Verley reduction: Pros and cons. *Appl. Catal. A Gen.* **2015**, *493*, 112–120. [CrossRef]
35. Van Der Graaff, W.N.; Li, G.; Mezari, B.; Pidko, E.A.; Hensen, E.J. Synthesis of Sn-Beta with Exclusive and High Framework Sn Content. *ChemCatChem* **2015**, *7*, 1152–1160. [CrossRef]
36. Emeis, C.A. ChemInform Abstract: Determination of Integrated Molar Extinction Coefficients for IR Absorption Bands of Pyridine Adsorbed on Solid Acid Catalysts. *J. Catal.* **1993**, *141*, 347–354. [CrossRef]
37. Luo, H.Y.; Lewis, J.D.; Román-Leshkov, Y. Lewis acid zeolites for biomass conversion: Perspectives and challenges on reactivity, synthesis, and stability. *Annu. Rev. Chem. Biomol. Eng.* **2016**, *7*, 663–692. [CrossRef]
38. Saikia, K.; Rajkumari, K.; Moyon, N.S.; Basumatary, S.; Halder, G.; Rashid, U.; Rokhum, S.L. Sulphonated biomass-based catalyst for solketal synthesis by acetalization of glycerol–A byproduct of biodiesel production. *Fuel Process. Technol.* **2022**, *238*, 107482. [CrossRef]
39. Wadlinger, R.L.; Kerr, G.T.; Rosinski, E.J. Catalytic Composition of a Crystalline Zeolite, Modil Oil Corporation. U.S. Patent 3,308,069, 7 March 1967.
40. Sebakhy, K.O.; Vitale, G.; Pereira-Almao, P. Production of Highly Dispersed Ni within Nickel Silicate Materials with the MFI Structure for the Selective Hydrogenation of Olefins. *Ind. Eng. Chem. Res.* **2019**, *58*, 8597–8611. [CrossRef]
41. Sebakhy, K.O.; Vitale, G.; Pereira-Almao, P. Dispersed Ni-doped Aegirine Nanocatalysts for the Selective Hydro-genation of Olefinic Molecules. *ACS. Appl. Nano Mater.* **2018**, *1*, 6269–6280. [CrossRef]

42. El Hariri El Nokab, M. Formation and Structural Analysis of Ultra Low-Density Silica Based Aerogels. Master's Thesis, University of Siegen, Siegen, Germany, 2018. [CrossRef]
43. Asgar Pour, Z.; Koelewijn, R.; El Hariri El Nokab, M.; van der Wel, P.C.; Sebakhy, K.O.; Pescarmona, P.P. Binder-free Zeolite Beta Beads with Hierarchical Porosity: Synthesis and Application as Heterogeneous Catalysts for Anisole Acylation. *ChemCatChem* **2022**, *14*, e202200518. [CrossRef]
44. El Hariri El Nokab, M.; Sebakhy, K.O. Solid State NMR Spectroscopy a Valuable Technique for Structural Insights of Advanced Thin Film Materials: A Review. *Nanomater.* **2022**, *11*, 1494. [CrossRef]